J Electr Eng Technol.2015;10(1): 308-313
http://dx.doi.org/10.5370/JEET.2015.10.1.308

ISSN(Print) 1975-0102
ISSN(Online) 2093-7423

Inverse Scattering of Two-Dimensional Objects Using Linear Sampling Method and Adjoint Sensitivity Analysis

Ahmadreza Eskandari† and Mohammad Reza Eskandari*

Abstract – This paper describes a technique for complete identification of a two-dimensional scattering object and multiple objects immersed in air using microwaves where the scatterers are assumed to be a homogenous dielectric medium. The employed technique consists of initially retrieving the shape and position of the scattering object using a linear sampling method and then determining the electric permittivity and conductivity of the scatterer using adjoint sensitivity analysis. Incident waves are assumed to be TM (Transverse Magnetic) plane waves. This inversion algorithm results in high computational speed and efficiency, and it can be generalized for any scatterer structure. Also, this method is robust with respect to noise. The numerical results clearly show that this hybrid approach provides accurate reconstructions of various objects.

Keywords: Inverse scattering, Microwave imaging, Linear Sampling Method (LSM), Adjoint Sensitivity Analysis (ASA).

1. Introduction

The imaging of scattering objects using microwaves is a major problem which is intensely investigated in the field of science and technology. This kind of imaging is implemented using an electromagnetic inverse scattering technique which involves the determination of geometrical and physical properties of a scatterer, such as position, size, shape, permittivity, conductivity, and permeability, from the measurements of the scattered EM fields resulting from the interaction of known incident waves with the unknown object [1-3]. This technique has many applications ranging from nondestructive testing and evaluation to medical imaging and from civil engineering to target identification [4, 5].

Numerical methods employed for solving inverse scattering problems can be grouped into two categories, i.e. qualitative and quantitative approaches [6, 7]. The singular source method [8], the factorization method (FM) [9] and the sampling method (SM) or the linear sampling method (LSM), are examples of qualitative methods. The LSM, introduced by Colton & Kirsch (1996), is an effective method to tackle the problem of reconstructing the shape of the unknown scatterer. This method does not require a priori knowledge on the scatterer's profile; however the physical properties, such as electrical permittivity value, of a penetrable scatterer cannot be calculated by using it [10-14]. There are also various quantitative methods used to reconstruct the scatterer, i.e. the nonlinear and linear approximation methods. Although these methods are capable of reconstructing the scatterer with high precision unfortunately they require a great deal of iterations to improve the initial guess [7, 11] and thus are very time consuming. Hence this makes the two quantitative methods undesirable.

In the last few years, there has been a concerted effort in developing hybrid strategies aimed at combining the positive features of two or more methods [15-18]. The basic idea involves combining the sampling methods with quantitative methods [15, 16]. In this paper, the complete identification of various scattering objects in free space is investigated. The imaging process is composed of two principle stages. In the first stage, the shape and the position of scatterers are reconstructed from the measured scattered field by using Linear Sampling Method (LSM). In the second stage, the Adjoint Sensitivity Analysis (ASA) is applied to determine the dielectric properties of the scatterers. This approach is an intelligent (not a stochastic optimization) method and it is technically correct and well organized. Previous theoretical investigations of such hybrid techniques have focused on combining the sampling methods with stochastic optimization methods [15, 18]. But these methods are rather slow in terms of computation and require a long time to reach the approximate solution. It should be mentioned that developing hybrid strategies for non-homogenous models is complex and practically impossible.

The paper is organized as follows. In Section 2 and 3, the mathematical details of the two-stage approach are discussed. The numerical examples are given in Section 4, followed by the complete reconstruction of scattering objects. Finally, Section 5 draws some conclusions.

† Corresponding Author: Department of Electrical Engineering, College of Engineering, East Tehran Branch, Islamic Azad University, Tehran, Iran. (areskandari@iauet.ac.ir)
* Electrical and Computer Engineering Department, Isfahan University of Technology, Isfahan, Iran. (mr.eskandari@ec.iut.ac.ir)
Received: January 10, 2014; Accepted: August 13, 2014

2. Linear Sampling Method

Our primary purpose is to reconstruct the shape of the scatterer by assuming a known far-field pattern u^∞ for every $\hat{x}, \hat{d} \in \Omega$ and constant wave number k. In the range of the resonance frequency the problem is solved using a sampling method. The principle of this technique is based on solving the Fredholm integral equation of the first kind ($Fg = \varphi$), as follow: [10, 11]

$$\mathrm{F}g(\hat{\mathrm{x}}) = \int_\Omega u^\infty(\hat{x}, \hat{d}) g(\hat{d}) d\Gamma(\hat{d}) = e^{jk\hat{x}.\hat{d}}, \quad \hat{x} \in \Omega \tag{1}$$

in which F is known as the far-field operator and u^∞ is the far-field pattern for the incident wave $u^i = e^{-jk\hat{x}.\hat{d}}$. A question raised is why and how the integral equation $Fg = \varphi$ will help to reconstruct the shape and the position of the scatterer D. Actually, Colton [10] has provided answers to this question.

3. Adjoint Sensitivity Analysis

In the previous subsection, the reconstruction method for the shape and the position of the scatterer was described. In many of the practical applications there is need to identify target material including electric permittivity and electric conductivity. Even by assuming that these parameters are constant or in other words the scatterer is homogenous, the ill-posedness and non-linearity of the problem will not change, and finding the material of scatterer has its own complications and difficulties. This problem is due to the errors that exist in reconstructing the shape and the position of the scatterer. These errors cause an inaccurate shape reconstruction of the scatterer. Therefore, by using a shape like $\tilde{D}$ similar to the actual shape of the scatterer D, its material properties are reconstructed. One of the methods to find the physical properties of the scatterer is by means of optimization stochastic algorithms, which takes up a long time to solve. In this section a logical and an appropriate solution is presented which is referred to as the Adjoint Sensitivity Analysis (ASA) [17, 19]. The ASA needs far less computational time in comparison to the stochastic methods. It presents an approximation solution based on the variations applied on the physical properties of the scatterer.

Since the scatterer is lossy, the relative complex permittivity is determined as $\zeta = \varepsilon_r - j\varepsilon_r'$, in which the imaginary section of ζ is calculated from: $\varepsilon_r' = \sigma/\omega\varepsilon_0$, where σ is the electric conductivity, and ε_0 is the electric permittivity of free space. If a variation $\delta\zeta$ is applied to parameter ζ, the electric fields inside and outside of the scatterer, will change and these variations will be correspondent to the equations below (these equations are obtained from Maxwell equations, the discontinuity conditions and the Sommerfeld radiation condition):

$$\nabla^2 \delta u^{ext} + k^2 \delta u^{ext} = 0 \quad \text{on} \quad R^2 \setminus \bar{D} \tag{2a}$$

$$\nabla^2 \delta u^{\mathrm{int}} + k^2 \zeta \delta u^{\mathrm{int}} = -k^2 \delta\zeta\, u^{\mathrm{int}} \quad on \quad D \tag{2b}$$

$$\delta u^{ext}\Big|_{\partial D^+} = \delta u^{\mathrm{int}}\Big|_{\partial D^-}, \quad \frac{\partial \delta u^{ext}}{\partial n}\bigg|_{\partial D^+} = \frac{\partial \delta u^{\mathrm{int}}}{\partial n}\bigg|_{\partial D^-} \tag{2c}$$

$$\lim_{|\vec{x}|\to\infty} \sqrt{|\vec{x}|}\left(\frac{\partial \delta u^s}{\partial |\vec{x}|} + jk\delta u^s\right) = 0 \tag{2d}$$

where δu^{int} and δu^{ext} are the changes created in electric fields u^{int} and u^{ext}, respectively, and the term $\delta\zeta\,\delta u^{\mathrm{int}}$ is ignored.

Assume that L is the direct scattering operator, and in (3) it takes the space of the incident field to the space of the scattered field:

$$L(u^i) = u^s \tag{3}$$

It is proven in [11] that the scattered field u^s can be calculated uniquely from the far-field pattern u^∞. Therefore, the far-field operator (L_∞) is defined as:

$$L_\infty(u^i) = u^\infty \tag{4}$$

Considering this definition and (3), the variations in the scattered fields may be written as:

$$L_\infty\left(\frac{\delta\zeta}{\zeta - 1} u^{\mathrm{int}}\right) = \delta u^\infty \tag{5}$$

This equation basically shows the variations of the scattered field in relation to the variations of the electric permittivity. In order to decrease the difference between the actual value and the measured value of the far-field pattern, we use the least square method. For this reason, cost function J is defined as:

$$J := \frac{1}{2}\left\| u^\infty - u^{meas} \right\|^2_{L^2(\Omega)} \tag{6}$$

where squared norm is defined as: $\|f\|^2_{L^2(\Omega)} := \int_\Omega f^2 d\Gamma$. By derivation from (6), we have:

$$dJ = \mathrm{Re}\left\{ \left\langle \delta u^\infty, u^\infty - u^{meas} \right\rangle_{L^2(\Omega)} \right\} \tag{7}$$

where inner product is defined as: $\langle f, g \rangle_{L^2(\Omega)} := \int_\Omega f.g d\Gamma$. By placing δu^∞ from (5) into (7), we have:

$$dJ = \mathrm{Re}\left\{\left\langle \frac{\delta\zeta}{\zeta-1}u^{\mathrm{int}}, L_{\infty}^{*}\left(u^{\infty}-u^{meas}\right)\right\rangle_{L^2(\Omega)}\right\} \quad (8)$$

for which L^* is the adjoint of the field operator L. In order to have negative variations for function J, $\delta\zeta$ is chosen to be:

$$\delta\zeta = \left\langle \beta L_{\infty}^{*}\left(u^{\infty}-u^{meas}\right), \frac{u^{\mathrm{int}}}{\zeta-1}\right\rangle_{L^2(D)} \quad (9)$$

where β is an arbitrary positive factor that affects the convergence speed of ASA. The smallness of β value has slowed down the convergence speed of ASA. Thus, it is better that β is chosen as the highest possible value so that ASA converges. By considering this point, the variations of β, will not have a tangible effect in ζ. However, by this choice of $\delta\zeta$ in (9), dJ becomes a negative value and J decreases. If these stages are repeated consecutively, the parameter ζ will converge to an optimum value.

4. Simulation Results

In this section the numerical results of three different structures will be presented. In all of the results presented the physical dimensions and distances have been normalized. As mentioned before the algorithm applied includes two stages: first, by the means of LSM the shape and the position of the scatterer are determined, and in the second stage the relative complex permittivity is calculated using ASA. In LSM, there is no need to solve the direct problem, but in the second stage it is considered as an optimization method. Therefore the direct problem has to be solved according to the number of incident waves. To decrease the amount of computations in this stage one incident wave is used.

In the simulations, $\|g\|$ is a characteristic function of the target and the boundary of the shape can be reconstructed by drawing an appropriate level. Also by choosing a specification function like $f(.)=-\log(.)$, the image of $\|g\|$ ($f(\|g\|)$) can be drawn so that the shape of the scatterer could be clearer.

In the simulations, sampling has been done uniformly on the far-field pattern. The far-field pattern is computed for the case where the number of the incident angles is equal to *n*, and their incident direction and measured direction are the same. Therefore:

$$k_i = k_s = \left[\cos(i\pi/n), \sin(i\pi/n)\right], \quad i = 0,\ 1,\ 2, ..., n \quad (10)$$

Forward scattering data is produced by using an integral equation on the scatterer (D region). This integral equation is referred to in [19]. The produced fields from this integral equation are used both in the LSM approach and in the iteration stages of the ASA method. In solving the mentioned integral equation, the moment method is used for discretization of the D region [19, 20]. The basic functions in our simulations are chosen to be a rectangular pulse. In all examples, the discretization is rectangular and the maximum value of the elements length is chosen to be $\lambda/10$.

4.1 Dielectric objects

The second example is relative to a U-shaped scattering object, as shown in Fig. 2. This is a homogeneous dielectric scatterer which has a relative complex permittivity equal to $\zeta = 10 - j5$ ($\varepsilon_r = 10$, $\varepsilon_r' = 5$). Also, it is assumed that the wavelength of the incident field is equal to 2π ($\lambda = 2\pi$ or *k*=1). The Tikhonov regularization parameter (α) is calculated by Morozov's discrepancy principle [21] and it is equal to 6.17×10^{-8}. Fig. 2 shows the result of the reconstructed shape of this scatterer qualitatively.

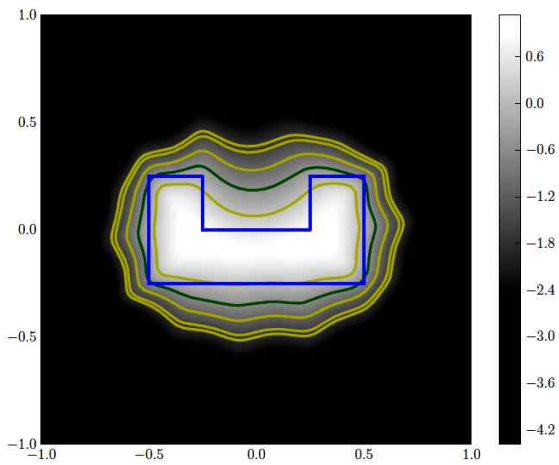

Fig. 2. Shape and Position Reconstruction of U-shaped homogeneous dielectric scatterer by LSM

Fig. 3 shows the detection of the material of the scatterer by using ASA. This figure shows the reconstruction of the real and imaginary parts of the relative complex permittivity in 180 iterations, which converges to 9.16 and 4.83, respectively.

4.2 Dielectric object with the presence of noise

The most important problem in solving ill-posed problems including the inverse scattering of electro-magnetic waves is the instability of the results due to the presence of noise. For this reason, in order to investigate the effect of noise on the far-field pattern and to evaluate the stability of the used method for detection of the scatterer, we use a uniform distribution function for noise with a 0.05 amplitude and a zero average, shown as

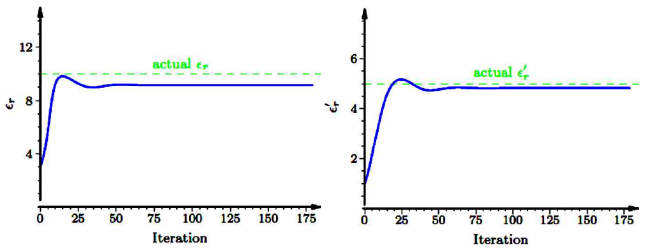

(a) (b)

Fig. 3. Reconstruction of the relative complex permittivity related to a U-shaped homogeneous dielectric scatterer by using ASA: (a) reconstruction of the real part; (b) reconstruction of the imaginary part

$N(0,0.05)$. The signal-to-noise power ratio (SNR) is defined as: $SNR = 10\log\left(\frac{E_{signal}}{E_{noise}}\right)$, where E_{signal} and E_{noise} are respectively the signal energy and the noise energy. The signal in this expression implies the values of the scattered field. With the above assumption for the noise, the SNR is calculated to be 30dB.

Figs. 4 and Fig. 5 show the results of this effect in reconstructing the scatterer. The topology of the actual scatterer is heart shaped with a relative complex permittivity equal to $\zeta = 10 - j5$. Without the effect of noise, the shape and the position of scatterer have been constructed in Fig. 4(a). The appropriate level of $-\log\|g\|$ is chosen to be -0.398. The relative complex permittivity converges to $9.89 - j4.94$ as depicted in Figs. 5(a) and (b). With the presence of noise ($SNR \cong 30dB$), the shape and the position of scatterer have been constructed in Fig. 4(b), where ζ converges to $9.37 - j4.62$ as depicted in Figs. 5(c) and (d). In Fig. 4(b), an appropriate level of $-\log\|g\|$ is chosen to be -0.176. In this example, the Tikhonov regularization parameter (α) that have been calculated, are equal to 1.21×10^{-8} and 1.236×10^{-2} for Figs. 4(a) and (b), respectively. Also, the β parameter that has been chosen is equal to 210.

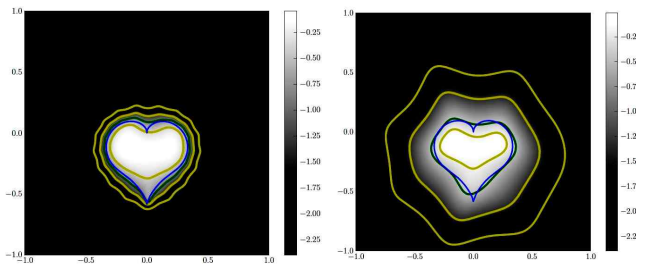

(a) (b)

Fig. 4. Shape reconstruction results of the heart shaped scatterer with absence and presence of noise: (a) without the effect of noise, (b) with the presence of noise (SNR=30dB).

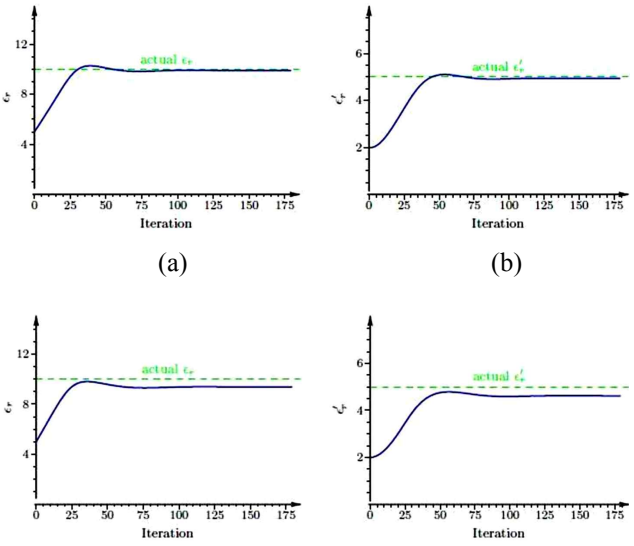

(a) (b)

(c) (d)

Fig. 5. Reconstruction results of the relative complex permittivity related of the heart shaped scatterer: (a) reconstruction of the real part of the relative complex permittivity which converges to 9.89 without the effect of noise; (b) reconstruction of the imaginary part of the relative complex permittivity which converges to 4.94 without the effect of noise; (c) reconstruction of the real part of the relative complex permittivity which converges to 9.37 with the presence of noise (SNR=30dB), and (d) reconstruction of the imaginary part of the relative complex permittivity which converges to 4.62 with the presence of noise (SNR=30dB).

4.3. Dielectric multiple objects

The third example is relative to two separate scattering objects with different permittivity and conductivity in free space, as shown in Fig. 6. In fact, the shapes of the actual scatterers have been shown by two closed lines (green and blue). These objects are homogeneous dielectric scatterers which have relative complex permittivity equal to $\xi_1 = 6 - 2j$ and $\xi_2 = 8 - 3j$ for green and blue closed lines, respectively. Fig. 6 shows the result of the reconstructed shape of these scatterers qualitatively. Also, it is assumed that the wavelength of the incident field is equal to 2 ($\lambda = 2$ or $k = \pi$). Figs. 7 and Fig. 8 show the detection of the materials of the scatterers by using ASA. Fig. 7 shows the reconstruction of the real and imaginary parts of the relative complex permittivity of the green line scaterrer in 180 iterations, which converges to 5.77 and 2.07, respectively. Fig. 8 shows the reconstruction of the real and imaginary parts of the relative complex permittivity of the blue line scaterrer in 180 iterations, which converges to 7.73 and 2.72, respectively.

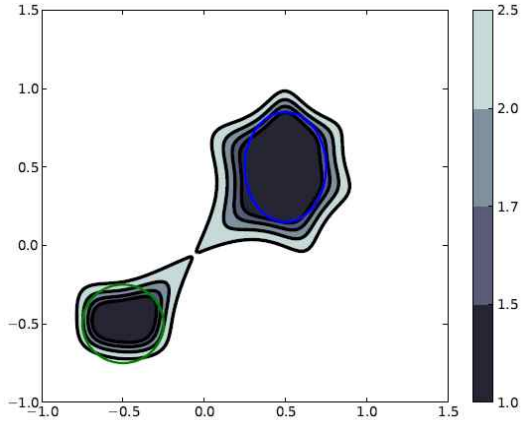

Fig. 6. Shape reconstruction of two separate scattering objects with different permittivity and conductivity in free space by using LSM ($k = \pi$).

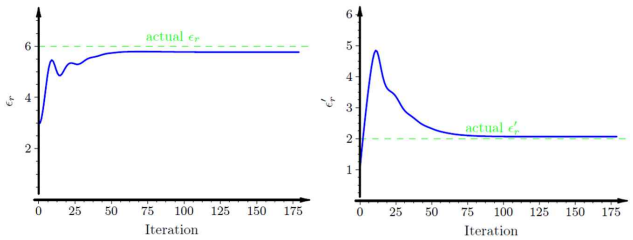

(a) (b)

Fig. 7. Relative complex permittivity reconstruction of the scatterer (green closed line) by using ASA: (a) reconstruction of the real part of ζ which converges to 5.77; (b) reconstruction of the imaginary part of ζ which converges to 2.07.

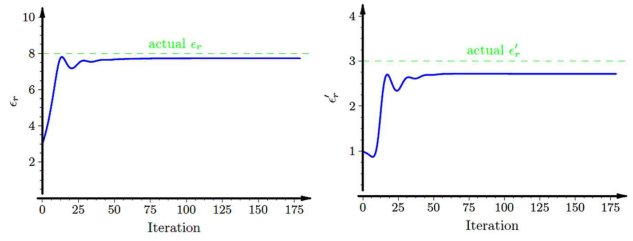

(a) (b)

Fig. 8. Relative complex permittivity reconstruction of the scatterer (blue closed line) by using ASA: (a) reconstruction of the real part of ζ which converges to 7.73; (b) reconstruction of the imaginary part of ζ which converges to 2.72

5. Conclusion

A complete reconstruction of 2D various scattering objects at microwave frequency was described using an algorithm combining linear sampling method with sensitivity analysis. The LSM was proposed because it can be applied to an extremely wide class of scatterers without any a priori information. The ASA was used to measure the sensitivity rate of the adjoint field operator versus the relative complex permittivity of the scatterer. The advantage of this hybrid approach is its high computational speed, efficiency, and stability. Furthermore, the inversion algorithm described can be generalized for other scatterer structures. Numerical results are used to validate the described technique. This approach can be expanded to be used for 3D scatterers, and it is suitable for practical implementation.

Acknowledgements

This research work has been financially supported by East Tehran Branch, Islamic Azad University, Tehran, Iran.

References

[1] Catapano, I., Crocco, L., and Isernia, T.: "Improved sampling methods for shape reconstruction of 3-D buried targets", IEEE Transaction on Geoscience and Remote Sensing, 2008, 46, (10), pp. 3265-3273.

[2] Eskandari, M., and Safian R.: "Inverse scattering method based on contour deformations using a fast marching method", Inverse Problems (IOP), 2010, 26, (9), 19.

[3] Abubakar, A., P. M. Van deng Berg and S. Y. Semenov, "Two- and Three-Dimensional Algorithms for Microwave Imaging and Inverse Scattering", J. of Electromagn. Waves and Appl., Vol. 17, No. 2, 2003.

[4] Benedetti, M., Donelli, M., Martini, A., Pastorino, M., Rosani, A., and Massa, A.: "An innovative micro-wave imaging technique for nondestructive evalution: Applications to civil structures monitoring and biological bodies inspection", IEEE Trans. Instrum. Meas., 55, pp.1878-1884, 2006.

[5] Fischer, C., Herschlein, A., Younis, M., and Wiesbeck, W.: "Detection of antipersonnel mines by using the factorization method on multistatic ground-penetrating radar measurements", IEEE Trans. Geosci. Remote Sens., Vol. 45, No. 1, pp. 85-92, 2007.

[6] Pastorino, M.: "Stochastic optimization methods applied to microwave imaging: a review", IEEE Trans. Antennas Propag., Vol. 55, pp.538-548, 2007.

[7] Pastorino, M., "Microwave Imaging", John Wiley & Sons, 2010.

[8] Fotouhi, M., & M. Hesaaraki., "The singular sources method for an inverse problem with mixed boundary conditions" Journal of Mathematical Analysis and Applications, Vol. 306, No. 1, 122-135, 2005.

[9] Kirsch, A., "The factorization method for Maxwell's equations", Inverse Problems (IOP), Vol. 20, No. 6, 117-134, 2004.

[10] Colton, D., and Kirsch A. "A simple method for

solving inverse scattering problems in the resonance regions", Inverse Problems, Vol. 13, pp. 383-393, 1996.
[11] Colton D., Haddar H., and Piana M. "The linear sampling method in inverse electromagnetic scattering theory", Inverse Problems (IOP), Vol. 19, No. 1, 105-137, 2003.
[12] Cakoni, F., Colton, D., and Haddar, H.: "The linear sampling method for anisotropic media", Journal of Computational and Applied Mathematics, Vol. 146, 285-299, 2002.
[13] Colton D., and Kress R.: "Using fundamental solutions in inverse scattering theory", Inverse Problems, Vol. 22, 285-299, 2006.
[14] Li, G.H., Zhao, X., and Huang, K.M.: "Frequency dependence of image reconstruction of linear sampling method in electromagnetic inverse scattering", Progress In Electromagnetics Research Symposium Proceedings, Xi'an, China, pp. 611-614, 2010.
[15] Brignone, M., Bozza, G., Randazzo, A., Piana, M., and Pastorino, M.: "A Hybrid approach to 3D microwave imaging by using linear sampling and ACO", IEEE Transaction Antenna and Propagation, Vol. 56, No. 10, 3224-3232, 2008.
[16] Eskandari A. R., M. Naser-Moghaddasi, and B.S. Virdee, "Target Identification Enhancement using a Combination of Linear Sampling Method and Adjoint Sensitivity Analysis", IET Microwave, antenna & Propagation, Vol. 6, No. 4, 461-469, 2012.
[17] A. Semnani and M. Kamyab, "An Enhanced Method for Inverse Scattering Problems Using Fourier Series Expansion in Conjunction with FDTD and PSO", Progress In Electromagnetics Research, PIER Vol. 76, 45-64, 2007.
[18] Bozza, G., Brignone, M., Pastorino, M., Piana, M., and Randazzo, A.: "An inverse scattering based hybrid method for the measurement of the complex dielectric permittivities of arbitrarily shaped homogenous targets", Proc. IEEE Instrumentation and Measurement Technology Conf. I2MTC '09, 719-723, 2009.
[19] Harrington, R. F., Field Computations by Moment Methods, New York: MacMillan, 1968.
[20] Gibson, W. C., The Method of Moments in Electromagnetics, Chapman & Hall/CRC, 2008.
[21] Grinberg N., Obstacle visualization via the factorization method for the mixed boundary value problem", Inverse Problems, Vol. 18, 1687-1704, 2002.

Ahmadreza Eskandari He received B.S and M.S. degrees in electrical engineering from Sharif University of Technology, Tehran, Iran, in 2002 and 2005, respectively, and the Ph.D. degree in electrical engineering from the Science and Research Branch, Islamic Azad University, Tehran Iran, in 2012. Currently, he is an Assistant Professor in the Department of Electrical Engineering, East Tehran Branch, Islamic Azad University, Tehran, Iran. His research interests are inverse scattering, microwave circuits and wave propagation.

Mohammad Reza Eskandari He received the B.S. and M.S degrees in electrical engineering from Isfahan University of Technology (IUT), Isfahan, Iran, in 2007 and 2009, respectively. He is currently working toward the Ph.D. degree at the Department of the Electrical and Computer Engineering, IUT. His research interests include computational electromagnetics, microwave imaging, inverse scattering theory, electromagnetic scattering and wave propagation.